RATE COEFFICIENTS FOR THE REACTION OF CHLORINE ATOMS WITH $FS(O_2)O$ AND $FS(O_2)OCl$ AT 298 K

Tucceri, M.E.; Castellano, E; Croce, A.E; Cobos, C.J.*

Instituto de Investigaciones Fisicoquímicas Teóricas y Aplicadas (INIFTA),
Departamento de Química, Facultad de Ciencias Exactas,
Universidad Nacional de La Plata, CONICET, CICPBA, Casilla de Correo 16,
Sucursal 4, (B1906ZAA) La Plata, Argentina.
Fax: +54 221 425 4642; *E-mail: cobos@inifta.unlp.edu.ar

Received June 30th, 2005. In final form July 26th, 2005.

Dedicated to the memory of the late Prof. Hans J. Schumacher on the occasion of his 100th birthday

Abstract

The kinetics of the recombination reaction $Cl + FS(O_2)O \rightarrow FS(O_2)OCl$ (1) has been studied by using an ArF excimer laser flash photolysis technique over the 25-950 mbar total pressure range of the bath gases He, N_2 and CF_4 at 298 K. The reaction was found to be essentially in the second-order regime. The derived limiting high-pressure rate coefficient is $k_{1,\infty}=(1.3\pm0.3)x10^{-10}$ cm³ molecule^{-1} s^{-1}. For the reaction $Cl + FS(O_2)OCl \rightarrow FS(O_2)O + Cl_2$ (2) a rate coefficient of $k_2 = (2.1\pm0.9)x10^{-11}$ cm³ molecule^{-1} s^{-1} was measured. The ratio between both rate coefficients of 0.16 agrees very well with data determined by Vasini and Schumacher. Quantum chemical calculations carried out at the G3MP2//B3LYP/6-311+G(3df) level of theory allow to determine an standard heat of formation of -136.5 kcal mol^{-1} for $FS(O_2)OCl$. Rate coefficient calculations in the framework of the phase space theory, performed on a G3MP2B3 electronic potential, indicate that central forces mainly dominate the present recombination reaction.

Resumen

La técnica de fotólisis flash con láser del excímero ArF se empleó para estudiar la cinética de la reacción de recombinación $Cl + FS(O_2)O \rightarrow FS(O_2)OCl$ (1) a presiones totales comprendidas entre 25 y 950 mbar de los gases He, N_2 y CF_4 y a 298 K. La reacción se encuentra esencialmente en la región de segundo orden. El coeficiente de velocidad determinado en el límite de alta presión es $k_{1,\infty}=(1,3\pm0,3)x10^{-10}$ cm³ molécula^{-1} s^{-1}. Se midió el coeficiente de velocidad $k_2=(2,1\pm0,9)x10^{-11}$ cm³ molécula^{-1} s^{-1} para la reacción $Cl + FS(O_2)OCl \rightarrow FS(O_2)O + Cl_2$ (2). El cociente entre ambos coeficientes de velocidad es 0,16 y se encuentra en muy buen acuerdo con el valor determinado por Vasini y Schumacher. Se calculó el valor -136,5 kcal mol^{-1} para el calor de formación estándar de $FS(O_2)OCl$ mediante el modelo G3MP2//B3LYP/6-311+G(3df). A partir de cálculos realizados mediante la teoría del espacio de las fases se encontró que la reacción de recombinación estudiada se encuentra dominada principalmente por fuerzas centrales.

Introduction

The recombination of radicals and the reverse simple bond dissociation reactions play a relevant role in many atmospheric [1,2] and combustion [3,4] mechanisms. Therefore, an understanding of the factors that dominate these rate coefficients with the goal of making reliable predictions of unavailable experimental data appears highly desirable. Although important progress has been done in this field due to the continuing improvements of the unimolecular rate theory, a considerable uncertainty remains because of the lack of knowledge of the molecular input data such as the details of the energy transfer processes or relevant parts of the potential energy surface. In this context, atom-diatomic radical chemical reactions present normally the simplest electronic potential features but usually require a large extrapolation of the falloff curve to obtain the limiting high pressure rate coefficients. At the next level of complexity, for atom-polyatomic radical reactions a more complicated anisotropic potential arises. In addition, the presence of a larger density of vibrational states shifts the high pressure region to lower total pressures allowing obtaining the high pressure rate coefficients more precisely.

In the present paper an experimental and theoretical study of the recombination reaction between chlorine atoms and fluorosulphonate radicals, $FS(O_2)O$, is considered. The formed product, chlorine fluorosulfate, $FS(O_2)OCl$, first prepared by Gilbreath and Cady [5], has been intensively employed as chlorinating, fluorosulfonating and oxidating agent. Although its chemistry has been considerably studied [6], only few kinetics studies of this interesting molecule have been reported.

The kinetics and the mechanism of the thermal reaction between the peroxydisulfuryl difluoride $FS(O_2)OO(O_2)SF$ and Cl_2 over the temperature range 373-408 K were reported by Vasini and Schumacher [7]. Under such experimental conditions the equilibrium established between $FS(O_2)OO(O_2)SF$ and the $FS(O_2)O$ radicals leads to a considerably high concentration of free radicals [8-11] which react with Cl_2 forming $FS(O_2)OCl$ and Cl atoms. Finally a competence between the reaction of Cl atoms with either $FS(O_2)O$ or $FS(O_2)OCl$ is operative. This mechanism explained well all experimental results [7]. More recently, a preliminary study of the kinetics of these reactions,

$$Cl + FS(O_2)O + M \rightarrow FS(O_2)OCl + M \qquad (1)$$

$$Cl + FS(O_2)OCl \rightarrow FS(O_2)O + Cl_2 \qquad (2)$$

was reported at room temperature [12]. This laser flash photolysis study confirmed the importance of these processes in the reaction mechanism of Vasini and Schumacher [7].

Continuing our time-resolved studies on the chemistry of $FS(O_2)O$ radicals, in the present work we investigate in more detail the kinetics of the reactions (1) and (2). Our goal was to analyze the falloff behavior of reaction (1) from both, the experimental and theoretical point of view. For this, we use the excimer laser flash photolysis technique complemented with quantum chemical and reaction rate theory calculations.

Experimental technique

The setup has been described in recent publications [13-15]. The $FS(O_2)O$ radicals were formed by $FS(O_2)OF$ photodissociation at 193 nm with an ArF excimer laser (Lambda Physik EMG 101 MSC). At this wavelength, $FS(O_2)OF$ exhibits an absorption cross section of 1.76×10^{-18} cm^2 $molecule^{-1}$ [16] and generate $FS(O_2)O$ and F atoms with unitary quantum yield [17]. These atoms afterwards react very fast with Cl_2 molecules added to the system according to

$$F + Cl_2 \rightarrow ClF + Cl \qquad (3)$$

Under the present conditions the F atoms are quantitatively converted into Cl atoms in about 200 ns [18]. Afterwards, the kinetics of reactions (1) and (2) was followed by monitoring the $FS(O_2)O$ concentration changes as a function of time. For this, the evolution of this only absorbing species was determined in real time by its absorption at 450 nm (spectral resolution, $\Delta\lambda$=1.5 nm). A crossed-beam configuration between the photolytic and the spectroscopic light beams was used. A xenon high-pressure arc lamp provides the probe light (Hanovia, 150 W). After passing through a reaction quartz cell of absorption path length of 2.5 cm, the probe light was focused onto the entrance slit of a prism double monochromator (Zeiss MM12) equipped with a photomultiplier tube (RCA, 1P28). The signals were recorded with a digital stored oscilloscope (LeCroy 9400) and further processed with a computer. A digital delay generator (SRS, DG535) was interfaced with the laser controlling system and the data acquisition system. Laser fluencies ranging from 10 to 40 mJ cm^{-2} were measured with a pyroelectric detector (Gentec, DE-500). The gases were handled in a Pyrex vacuum system, and the pressures measured with a pressure transducer (MKS Baratron, Type 310CA) and with a sensitive quartz spiral gauge. Typical $FS(O_2)OF$ and Cl_2 pressures ranging from 3 to 8 mbar were employed. The diluents bath gases were varied between 19-935 mbar (He), 11-785 mbar (N_2) and 16-940 mbar (CF_4). All experiments were performed at 298±2 K.

The $FS(O_2)OF$ was prepared by photolysis of F_2 in the presence of SO_3 [19], The other employed gases had the followed stated minimum purities: Cl_2, 99.9% (Matheson); He, 99.999% (Union Carbide); N_2, 99.99% (La Oxígena) and CF_4, 99.7% (Matheson).

Results and discussion

a) Experimental rate coefficients for reactions (1) and (2).

The $FS(O_2)O$ radical exhibits weak diffuse absorption bands at 1300-1400 nm and 720-840 nm and a discrete band with origin at 516 nm resulting from the C^2E-X^2A_2 transition [20]. The latter is partially overlapped by a fairly strong continuum that decreases in intensity between about 470 and 340 nm [16, 20, 21]. At the selected monitoring wavelength of 450 nm, the absorption cross section has been determined to be $(3.64 \pm 0.32) \times 10^{-18}$ cm^2 $molecule^{-1}$ [10].

Due to the fact that the $FS(O_2)O$ self-recombination reaction

$$FS(O_2)O + FS(O_2)O \rightarrow FS(O_2)OO(O_2)SF \quad (4),$$

is slow ($k_{4,\infty} = 4.5x10^{-14}$ cm^3 molecule^{-1} s^{-1} [10]) and the reaction

$$FS(O_2)O + Cl_2 \rightarrow FS(O_2)OCl + Cl \quad (5),$$

is extremely slow ($k_5=1.1x10^{-23}$ cm^3 molecule^{-1} s^{-1} [7]), the $FS(O_2)O$ can only react with the Cl atoms formed in reaction (3). A trace of the time evolution of $FS(O_2)O$ for a typical experiment is shown in Figure 1. The pronounced initial $FS(O_2)O$ decrease is almost exclusively ascribed to reaction (1). Afterwards, at above about 8 μs, the global rate of $FS(O_2)O$ consumption decreases strongly with time. This is interpreted considering the main participation of reaction (2) when $FS(O_2)OCl$ concentration increases due to reaction (1). It is important to note that reaction (6)

$$Cl + FS(O_2)OF \rightarrow FS(O_2)O + ClF \quad (6)$$

does not contribute to the reaction mechanism [12, 22]. Therefore, the time-dependent $FS(O_2)O$ concentrations were well interpreted with the mechanism formed by reaction (1) and (2). A typical fit is shown in Figure 1. In addition, the contribution of both reactions to the signal is also indicated. In fact, curve *A* corresponds to a pure second-order behavior similar to the reported for the reaction [23]

$$F + FS(O_2)O + M \rightarrow FS(O_2)OF + M \quad (7).$$

The abstraction reaction $F + FS(O_2)OF \rightarrow FS(O_2)O + F_2$ does not play any role. An activation energy of about 10 kcal mol^{-1} has been estimated for this process [23, 24]. On the other hand, the first-order signal denoted by *B* in Fig. 1, corresponds to the growing of $FS(O_2)O$ concentration by reaction (2). Similar signals have been monitored during the laser-induced temperature jump measurements of the $FS(O_2)OO(O_2)SF \leftrightarrow FS(O_2)O + FS(O_2)O$ equilibrium above 500 K [11]. The absorption signals were monitored up to about 200 μs, time at which a slight decrease of $FS(O_2)O$ concentration ascribed to reaction (4) has been observed. The $FS(O_2)O$ absorption vanished at about 30 ms [10].

The determined second-order rate coefficients for reaction (1) and (2) are listed in Table 1. For convenience, the analysis of reaction (2) is given first. The obtained average k_2 is

$$k_2 = (2.1 \pm 0.9) \times 10^{-11} \text{ cm}^3 \text{ molecule}^{-1} \text{ s}^{-1}$$

This value is 38% larger than the previously reported [12]. The difference is mostly attributed to the more accurate present numerical simulation.

Further evidence for the formation of Cl_2 by the abstraction of Cl atoms from other hypofluorites by Cl have been reported. In fact, in either the stationary photolysis of CF_3OCl or in the photolysis of Cl_2 in the presence of CF_3OCl, the reaction products CF_3OOCF_3 and Cl_2 are exclusively formed [25]. Similarly, large amounts of SF_5OOSF_5 and Cl_2 are generated by photolysis of SF_5OCl [26]. More recently, the relevant role that reaction $Cl + ClOClO_3 \rightarrow Cl_2 +$

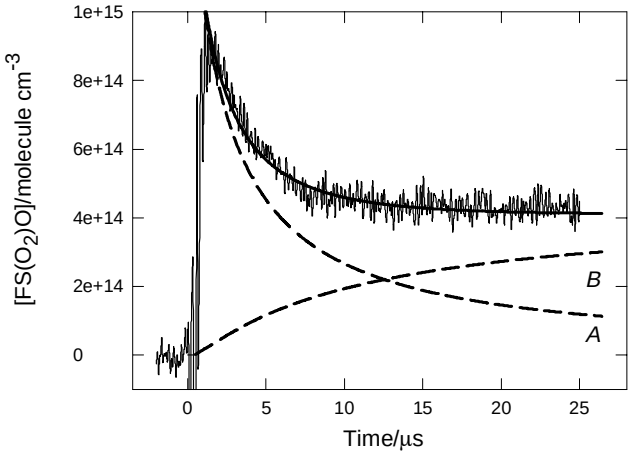

Figure 1. *Time-resolved $FS(O_2)O$ concentration detected at 450 nm following the 193 nm-photodissociation of 6.5 mbar of $FS(O_2)OF$ in the presence of 6.7 mbar of Cl_2 and 67.6 mbar of CF_4. The best fit was obtained with $k_1=1.3x10^{-10}$ cm³ molecule^{-1} s^{-1} and $k_2=2.4x10^{-11}$ cm³ molecule^{-1} s^{-1}. The dashed lines A and B are the results of the modeling described in the text.*

ClO_4 plays on the mechanism of the 366 nm photolysis of Cl_2 in the presence of $ClOClO_3$ has been demonstrated [27]. On an absolute basis, the present rate coefficient value for reaction (2) is comparable with those measured for other selected Cl abstraction reactions, i. e, $6.1x10^{-11}$ cm³ molecule^{-1} s^{-1} for $Cl + CH_3OCl \rightarrow Cl_2 + CH_3O$ [28, 29]; $4.3x10^{-11}$ cm³ molecule^{-1} s^{-1} for $Cl + C_4H_9OCl \rightarrow Cl_2$ + other products [29] and $1.5x10^{-11}$ cm³ molecule^{-1} s^{-1} for $Cl + FC(O)OCl \rightarrow Cl_2 + FC(O)O$ [30].

As observed in Table 1, the values of k_1 for M=He show a very small pressure dependence. This is more evident in Figure 2, where all measured rate coefficients are depicted. The analysis of these data is discussed below.

Table 1. *Measured second-order rate coefficients for reactions (1) and (2).*

Pressure (mbar)					k_1 (cm³ molecule^{-1} s^{-1})	k_2 (cm³ molecule^{-1} s^{-1})
$FS(O_2)OF$	Cl_2	He	N_2	CF_4		
3.3	4.8	18.6	—	—	$7.7x10^{-11}$	$2.8x10^{-11}$
5.9	8.2	32.1	—	—	$1.1x10^{-10}$	$1.5x10^{-11}$
5.9	8.0	131.9	—	—	$1.4x10^{-10}$	$1.2x10^{-11}$
3.1	3.1	399.3	—	—	$9.3x10^{-11}$	$3.7x10^{-11}$
7.2	7.0	934.9	—	—	$1.3x10^{-10}$	$2.1x10^{-11}$
6.1	6.9	—	10.9	—	$8.9x10^{-11}$	$1.9x10^{-11}$

5.3	6.8	—	784.0	—	$9.2x10^{-11}$	$2.7x10^{-11}$
6.5	3.5	—	—	31.4	$1.5x10^{-10}$	$1.6x10^{-11}$
3.3	3.3	—	—	33.8	$1.1x10^{-10}$	$3.8x10^{-11}$
6.5	3.5	—	—	65.2	$1.4x10^{-10}$	$2.0x10^{-11}$
6.5	6.7	—	—	67.6	$1.3x10^{-10}$	$2.4x10^{-11}$[o]
6.5	3.4	—	—	133.0	$1.4x10^{-10}$	$1.6x10^{-11}$
3.1	3.3	—	—	134.2	$1.5x10^{-10}$	$3.1x10^{-11}$
6.5	3.4	—	—	210.1	$1.6x10^{-10}$	$1.7x10^{-11}$
6.1	6.6	—	—	272.3	$1.4x10^{-10}$	$1.8x10^{-11}$
6.5	3.5	—	—	351.9	$1.3x10^{-10}$	$6.9x10^{-12}$
3.3	3.3	—	—	465.1	$1.6x10^{-10}$	$1.0x10^{-11}$
6.8	6.7	—	—	942.2	$1.3x10^{-10}$	$1.5x10^{-11}$

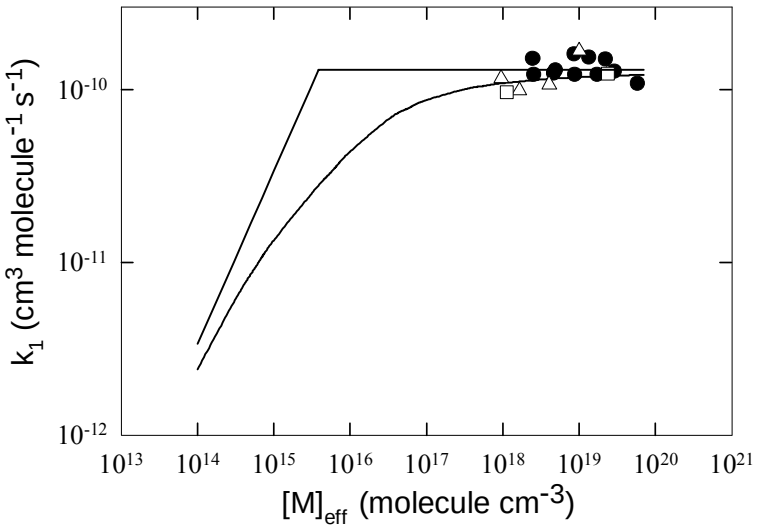

***Figure 2**. Falloff curve of the reaction (1) for the bath gases He (Δ), N_2 (□) and CF_4 (●). $[M]_{eff}=[He]+1.2[N_2]+2.5[CF_4]+2.7[FS(O_2)OF]+2.5[Cl_2]$ (see text). The solid line through the data is the fit with the formalism described in the text. The solid straight lines correspond to the limiting low- and high pressure rate coefficients.*

b) Quantum chemical calculations

To perform the theoretical kinetic calculations for reaction (1) described in the next section, relevant molecular data for the participant species are required. To complement the available

experimental information, quantum chemical calculations were carried out using the Gaussian 03 program package [31]. The molecular structure and the harmonic vibrational frequencies of $FS(O_2)OCl$ were calculated using the hybrid B3LYP density functional which employs the Becke´s three parameter exchange functional [32,33] coupled to the nonlocal correlational functional of Lee, Yang and Parr [34]. The large 6-311+G(3df) Pople´s basis set was selected for all calculations. The energetic was computed, at high level of theory, using the G3MP2B3 *ab initio* model chemistry [35]. A modified version G3MP2//B3LYP/6-311+G(3df) that uses B3LYP/6-311+G(3df) calculations instead of B3LYP/6-31G(d) to estimate the geometry and the vibrational frequencies (without scaling) was also employed [36]. The calculated molecular structure for $FS(O_2)OCl$ agrees very well with the one measured in gas electron diffraction (GED) experiments [37]. The small mean absolute deviations of 0.019 Å for the bond distances and 1.3° for the bond angles indicate the very good agreement found here. The calculations predicts a gauche conformation with τ(FSOCl)=70.9° as the more stable conformation. The experimental GED value is 69° [37]. From the theoretical structure we derive the following rotational constants: A=0.163, B=0.0580 and C=0.0575 cm^{-1}. On the other hand, the computed vibrational frequencies of 1484, 1244, 823, 794, 694, 561, 516, 470, 366, 351, 191 and 97 cm^{-1} compare very well with the experimental values of 1485, 1246, 855, 832, 704, 571, 530, 490, 387, 359, 208 and 95 cm^{-1} [37]. The mean absolute deviation between both sets of values is 19 cm^{-1}. Similar values of 12, 13 and 18 cm^{-1} were obtained at the B1LYP, B3PW91 and mPW1PW91 levels of theory. The calculated and experimental values for the O-Cl stretching mode are 694 and 704 cm^{-1} respectively.

The kinetics analysis described below requires the knowledge of the $FS(O_2)OCl$ internal rotational motions. For this, molecular conformations were fully optimized for both the gauche and trans (τ(FSOCl)=180°) conformations and for intermediate structures of $FS(O_2)OCl$. The resulting rotational potential evaluated at the B3LYP/6-311+G(3df)//B3LYP/6-311+G(d) level is shown in Figure 3. More accurate G3MP2B3 calculations carried at selected points of the potential are also indicated. The highest electronic barrier was determined to be V_0=7.1 kcal mol^{-1}. The associated reduced moment of inertia is I_r=4.57 amu $Å^2$. The $FS(O_2)O$-Cl rotational barrier is similar to those calculated with the B3LYP/6-31G(d,p) functional for the Cl-Cl eclipsed structures of $CHCl_2OCl$, 8.08 kcal mol^{-1} and CCl_3COCl, 6.30 kcal mol^{-1} [38]. Our best calculations lead to a barrier of 1.2 kcal mol^{-1} for the conversion between the trans and gauche structures. By comparison, at the HF/6-31G(d) level a value of 2.1 kcal mol^{-1} has been reported [37].

The heat of formation of $FS(O_2)OCl$ was estimated from the calculated total atomization energy, i.e. the energy required to dissociate the molecule into its separate atoms. The value calculated at the G3MP2//B3LYP/6-311+G(3df) level of 416.2 kcal mol^{-1} leads to a heat of formation of $\Delta H^o_{f,298}$=-128.6 kcal mol^{-1}. It was afterwards corrected by using a recently implemented bond additivity correction (BAC) procedure [39]. This method involves atomic, molecular and pairwise bond corrections for the heat of formation. For the present case, the BAC is 8.2 kcal mol^{-1}, therefore the above heat of formation is reduced to $\Delta H^o_{f,298}$=-136.8 kcal mol^{-1}. Independent calculations, which rely on the construction of isodesmic reaction schemes, were also carried out. In this procedure, the heat of formation for the molecule of interest is evaluated by combining the computed enthalpy change of the selected reaction with well-established heats of formation for other reaction components. In this way, from the selected reaction

$$ClOH + FS(O_2)OH \rightarrow FS(O_2)OCl + H_2O,$$

the calculated ΔH^o=3.6 kcal mol^{-1} and the heats of formation of -17.9, -57.8 [1] and -180.0 [40] for ClOH, H_2O and $FS(O_2)OH$ respectively, we obtain the value $\Delta H^o_{f,298}$=-136.5 kcal mol^{-1} which agrees very well with the derived from atomization. This value together with the heats of formation values of Cl of 29.0 kcal mol^{-1} [1] and of $FS(O_2)O$ of -121.3 kcal mol^{-1} [13] yield a $FS(O_2)O$-Cl bond dissociation enthalpy of ΔH^o_{298}=44.2 kcal mol^{-1}. It is interesting to note that this value compares very well with the estimated by Vasini and Schumacher on kinetic grounds of 45 kcal mol^{-1} [7]. The potential energy features relevant in the theoretical interpretation of the kinetics of reaction (1) are discussed in the next section.

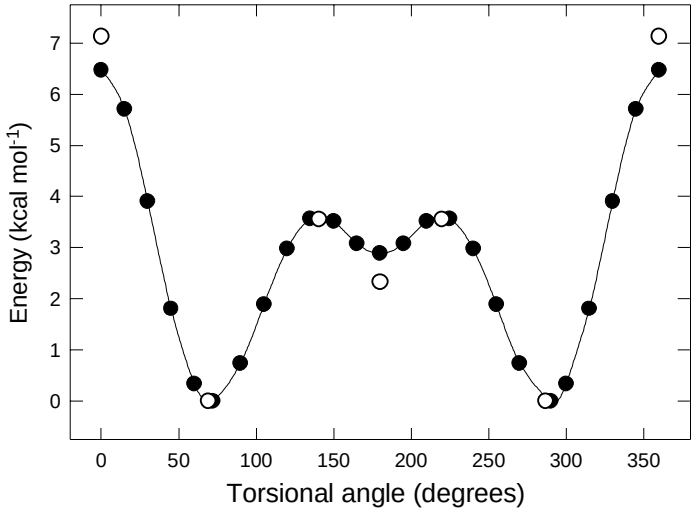

Figure 3. *Rotational potential for torsion around the O-Cl bond in $FS(O_2)OCl$. Calculations at the levels B3LYP/6-311+G(3df)//B3LYP/6-311+G(d) (●) and G3MP2B3 (o).*

c) Falloff curves and limiting low and high-pressure rate coefficients

To analyze the pressure dependence of the rate coefficients k_1, the falloff curve depicted in Figure 2 was employed. This curve shows the transition of k_1 from the low-pressure range, where it is proportional to the effective total pressure $[M]_{eff}$ (see below), $k_{1,0}$, to the high-pressure range, where it approaches the constant value $k_{1,\infty}$. The falloff curve was estimated by using the general expression [41]

$$k = k_\infty F^{LH}(k_0/k_\infty)\, F(k_0/k_\infty) \qquad (I)$$

The factor $F^{LH}(k_0/k_\infty) = \dfrac{k_0/k_\infty}{1+k_0/k_\infty}$ is the result of the simple Lindemann-Hinshelwood mechanism. Here, $k_0=\lim_{[M]\rightarrow 0} k([M])$ and $k_\infty=\lim_{[M]\rightarrow \infty} k([M])$ are pseudo-second order rate

coefficients. The broadening factor $F(k_0/k_\infty)$ accounts for corrections due to the energy and total angular momentum dependence of the excited species and for the multistep character of the energy transfer process assisted by collisions. This factor was estimated as [41, 42]

$$F(k_0/k_\infty) \approx F_{cent}^{1/\{1+[(\log(k_0/k_\infty)+0.2)/N(k_0/k_\infty)]^2\}} \quad \text{(II)}$$

$$F(k_0/k_\infty) \approx F^{WC}(k_0/k_\infty)\ F^{SC}(k_0/k_\infty) \quad \text{(III)}$$

$$F(k_0/k_\infty) \approx \beta_c^{0.14}\ S_K^{-0.62} \quad \text{(IV)}$$

where F^{WC}_{center} and F^{SC}_{center} are respectively the weak and the strong collision broadening factors and $N(k_0/k_\infty) \approx \{1.448\text{-}0.7780\log(k_0/k_\infty)+0.1067([\log(k_0/k_\infty)]^2\}(k_0/k_\infty)^{0.178}$ is a width function [42]. Weak collision effects are accounted for by the bath gas collision efficiencies β_c. At the phase space limit, the transitional modes exhibit rotational character therefore $S_K \approx 1+r/2$ [42]. Here r is the total number of external rotational modes of the reactants, i.e. for the present case r =3.

In the falloff curve of Figure 2, we define an effective pressure scale as $[M]_{eff}=\Sigma(\beta_{c,i}Z_{LJ,i}/\beta_{c,He}Z_{LJ,He})[M_i]$. The Lennard-Jones collision frequencies Z_{LJ} between the excited adduct $FS(O_2)OCl$ and a given bath gas were estimated, as usual, from Lennard-Jones parameters derived from the critical properties of the gases or from tabulated values [43]. The employed β_c values correspond to those determined for the similar reaction $F + FS(O_2)O + M \rightarrow FS(O_2)OF + M$, i.e., $\beta_c \approx 0.1$, 0.2 and 0.4 for M=He, N_2 and Cl_2 and $\beta_c \approx 0.5$ for CF_4 and $FS(O_2)OF$ [23]. Due to the fact that experimental rate coefficients are close to the high-pressure region, an estimation of the $k_{1,0}$ values for each bath gas was done. For this, the factorized expression given by the unimolecular rate theory was used [41, 44, 45]

$$k_0 = \beta_c(1/K_C)[M]Z_{LJ}\frac{\rho_{vib,h}(E_0)k_BT}{Q_{vib}}\exp\left(-\frac{E_0}{k_BT}\right)F_{anh}\ F_E\ F_{rot}\ F_{rotint} \quad \text{(V)}$$

The significance of the various factors and their values at 298 K are the following. $K_C = k_{-1}/k_1 = 1.99\times10^6$ cm^3 molecule^{-1} is the equilibrium constant evaluated with the above molecular properties of $FS(O_2)OCl$, the experimental vibrational frequencies [37] and the $FS(O_2)O$ rotational constants [13], $\rho_{vib,h}(E_0)=1.24\times10^8$ (kcal mol^{-1})$^{-1}$ is the harmonic vibrational density of states of $FS(O_2)OCl$ at the threshold energy $E_0 \approx \Delta H^\circ_0 = 42.9$ kcal mol^{-1} and $Q_{vib}=3.11$ the vibrational partition function of $FS(O_2)OCl$. The F factors take into account corrections for effects of anharmonicity $F_{anh}=1.15$, spread of internal energies $F_E=1.14$, external rotations $F_{rot}=11.79$, and internal rotations $F_{rot\ int}=7.62$. For M=He, using Z_{LJ}(He-$FS(O_2)OCl$)$=5.87\times10^{-10}$ cm^3 molecule^{-1} s^{-1} and $\beta_c=0.1$ we have $k_{1,0}=1.3\times10^{-26}$[He] cm^3 molecule^{-1} s^{-1}.

The curve depicted in Figure 2 was fitted to the experimental results using the equations (I) to (IV) with $[M]_{eff}=[He]+1.2[N_2]+2.5[CF_4]+2.7[FS(O_2)OF]+2.5[Cl_2]$ and the above $k_{1,0}$ value. The resulting limiting high pressure rate coefficient is

$$k_{1,\infty} = (1.3\pm0.3) \times 10^{-10} \text{ cm}^3 \text{ molecule}^{-1} \text{ s}^{-1}$$

The center of the falloff curve is defined as the concentration at which the limiting $k_{1,0}$ and $k_{1,\infty}$ intersect in Figure 2, that is, $[M]_{eff,c} \approx [CF_4]_c \approx 4\times10^{15}$ molecule cm$^{-3} \approx 0.2$ mbar. For He we have $[He]_c \approx 0.4$ mbar. These values contrast with those derived for the similar recombination reaction $F+FS(O_2)O+M \rightarrow FS(O_2)OF+M$ of $[CF_4]_c \approx 2.8$ mbar and $[He]_c \approx 7.6$ mbar [23]. For this process, falloff curves for M=He, N_2, CF_4 and SF_6 were derived between 298 and 378 K. From these curves, low pressure rate coefficients and a high pressure rate coefficient of $(7.6\pm1.0) \times 10^{-11}$ cm^3 molecule^{-1} s^{-1} were determined.

It should be noted that the present ratio $k_2/k_{1,\infty} = 0.16$ agrees very well with the value estimated at room temperature from the data of ref. 7 of 0.18. On the other hand, the large $k_{1,\infty}$ here obtained is similar to those measured for other Cl atom reactions. In fact, k_∞ values of 1.0×10^{-10}, 2.0×10^{-10}, 2.8×10^{-10} and 1.4×10^{-10} cm^3 molecule^{-1} s^{-1} have been measured respectively for the reactions of Cl with NO_2, C_2H_2, C_3H_6 and C_3H_8 [1, 2].

It appears interesting at this stage to interpret $k_{1,\infty}$ in terms of the reaction rate theory. For this, we use phase space theory (PST), which provides an upper limit to the rate coefficients [46-48]. Here the isotropic electronic potential V(r) along the minimum energy path determines the rate coefficients. The *ab initio* G3MP2B3 model was used to study the $FS(O_2)O$-Cl potential [35]. This potential was then improved by a BAC procedure [39]. The computed BAC-G3MP2B3 potential and a fit with the Morse function (in kcal mol^{-1}) $V(r)=46.8\{1-\exp[-2.74(r-1.736)]\}^2$ is given in Figure 4. These calculations also provide the effective rotational constants (in cm^{-1}), $B_{eff}(r)=[B(r)+C(r)]/2=5.597\times10^{-2}/[1+0.2435(r-1.736)+0.1637(r-1.736)^2]$, along the reaction coordinate. The PST rate coefficients were evaluated as

$$k_\infty(\text{PST}) = f_e \sum_{J=0}^{\infty} (2J+1) \int_{Eo(J)}^{\infty} W^{\#}(E,J) \exp\left(-\frac{E}{k_B T}\right) \frac{dE}{k_B T} \qquad \text{(VI)}$$

Here $f_e \approx 1/4$ is the electronic degeneracy factor. The J-dependence of the dissociation threshold energy $E_0(J)$ was computed from the maxima of the potential $V_{cent}(r)=V(r)+B_{eff}(r)[J(J+1)]$. The number of open channels W(E, J) was calculated with the expressions of ref. 49. The resulting value at 300 K of $k_{1,\infty}(\text{PST}) = 1.41\times10^{-10}$ cm^3 molecule^{-1} s^{-1} suggests that anisotropic forces play only a minor role. In fact, the rigidity factor estimated as $f_{rigid} = k_{1,\infty}/k_{1,\infty}(\text{PST}) \approx 0.9$ [48] shows that anisotropy effects arising from the angular forces in the transitional modes are very small.

To compare with the present system, calculations were also carried out for reaction (7). The computed BAC-G3MP2B3 electronic potential is depicted in Figure 4. As before, it was fitted with a Morse function with parameters $\beta=3.11$ Å^{-1} and $D_e=36.0$ kcal mol^{-1}, while $B_{eff}(r)$ was very well reproduced with the relationship $B_{eff}(r)=8.740\times10^{-2}/[1+0.1485(r-1.433)+0.0751(r-1.433)^2]$. From the calculated limiting high pressure rate coefficient of 1.10×10^{-10} cm^3 molecule^{-1} s^{-1}, a rigidity factor of about 0.7 is derived. For the sake of comparison, the related reactions $Cl + FC(O)O \rightarrow FC(O)OCl$ and $F + FC(O)O \rightarrow FC(O)OF$, recently studied in our laboratory, exhibit experimental rigidity factors of 0.72 [50] and 0.36 [14]. In both cases, the f_{rigid} values corresponding to the Cl atom reactions are larger than those obtained for F atoms reactions.

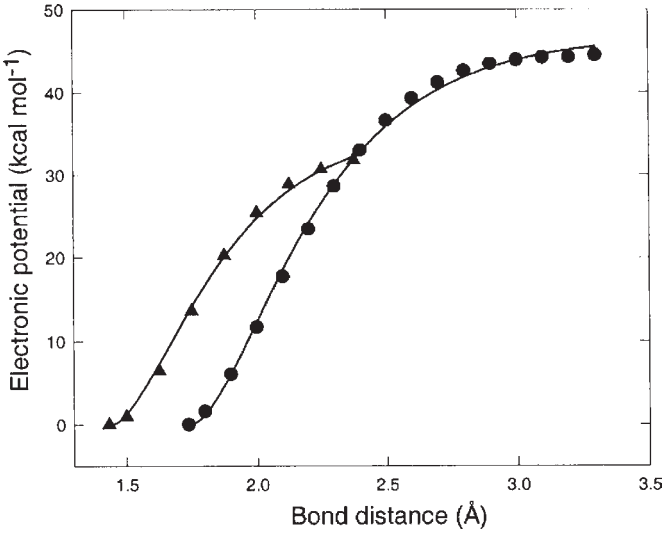

Figure 4. *Potential energy curves for $FS(O_2)OCl \rightarrow FS(O_2)O + Cl$ (●) and $FS(O_2)OF \rightarrow FS(O_2)O + F$ (▲) calculated at the BAC-G3MP2B3 level. The solid lines are the fits with Morse functions (see text).*

Conclusions

The 193-nm laser flash photolysis of $FS(O_2)OF$ in the presence of Cl_2 and the third-body gases He, N_2 and CF_4 has been investigated at room temperature. These experiments allow to directly determine the limiting high pressure rate coefficient of reaction $Cl + FS(O_2)O \rightarrow FS(O_2)OCl$ and the rate coefficient of the abstraction reaction $Cl + FS(O_2)OCl \rightarrow FS(O_2)O + Cl_2$. The combined rate coefficients agree very well with the results published thirty seven years ago by Vasini and Schumacher. Some molecular properties for $FS(O_2)OCl$ were derived at high quantum chemical levels and used in the theoretical kinetic interpretation of the recombination reaction. The performed analysis indicates that angular anisotropic forces play only a small role in the capture rate coefficient and thus the reaction is mostly dominated by the long-range attractive part of the potential energy surface.

Acknowledgements

This research project was supported by the Universidad Nacional de La Plata, the Consejo Nacional de Investigaciones Científicas y Técnicas (CONICET), the Comisión de Investigaciones Científicas de la Provincia de Buenos Aires (CICPBA) and the Max Planck Institute for Biophysical Chemistry Göttingen through the "Partner Group for Chlorofluorocarbons in the Atmosphere".

References

[1] Sander, S. P.; Friedl, R. R.; Golden, D. M.; Kurylo, M. J.; Huie, R. E.; Orkin, V. L.; Moortgat, G. K.; Ravishankara, A. R.; Kolb, C. E.; Molina, M. J.; Finlayson-Pitts, B. J.;

Chemical Kinetics and Photochemical Data for Use in Atmosferic Studies, NASA/ JPL Data Evaluation, JPL Publication 02-25 Evaluation No 14, February 2003. http://jpldataeval.jpl.nasa.gov/ .

[2] Atkinson, R.; Baulch, D. L.; Cox, R. A.; Crowley, J. N.; Hampson, R. F.; Hynes, R. G.; Jenkin, M. E.; Rossi, M. J.; Troe, J; *Atmos. Chem. Phys.* **2004**, *4*, 1461.

[3] Baulch, D. L.; Cobos, C. J.; Cox, R.A.; Frank, V; Hayman, G.; Just, Th.; Kerr, V; M; Murrells, T.; Pilling, M. J.; Troe, J.; Walker, J.; Warnatz, J. *J. Phys. Chem. Ref. Data* **1994**, *23*, 847.

[4] Baulch, D.L. Bowman, C. T.; Cobos, C.J.; Cox, R.A.; Just, Th.; Kerr, J. A.; Pilling, M.J.; Stocker, D.; Troe, J.; Tsang, W.; Walker, R. W; Warnatz, J. *J. Phys. Chem. Ref. Data*, **2005,** *34(3)*, 757.

[5] Gilbreath, W.; Cady, G. H. *J. Inorg. Nuclear Chem*. **1963**, *2*, 496.

[6] Schack, C. J.; Christe, K. O; *Israel J. Chem.* **1978**, *17*, 20.

[7] Vasini, E. J..; Schumacher, H. J. *Z. Physik. Chem. NF*, **1968**, *65*, 238.

[8] Dudley F. B.; Cady, G. H.; *J. Amer. Chem. Soc.* **1963**, *65*, 3375.

[9] Castellano, E.; Gatti, R.; Sicre, J. E.; Schumacher, H. J. *Z. Physik. Chem. NF*, **1964**, *42*, 174.

[10] Cobos, C. J.; Croce de Cobos, A. E.; Hippler, H.; Castellano, E. *J. Phys. Chem.* **1989**, *93*, 3089.

[11] Cobos, C. J.; Croce, A. E.; Castellano, E. *Int. J. Chem. Kinet.* **1990**, *22*, 289.

[12] Croce, A. E.; Cobos, C. J.; Castellano, E. *Chem. Phys. Lett.* **1989**, *158*, 157.

[13] Tucceri, M. E.; Badenes, M. P.; Croce, A. E.; Cobos, C. J. *Phys. Chem. Chem. Phys.* **2001**, *3*, 1832.

[14] Badenes, M. P.; Croce, A. E.; Cobos, C. J. *Phys. Chem. Chem. Phys.* **2004**, *6*, 747

[15] Tucceri, M. E.; Croce, A. E.; Cobos, C. J. *Chem. Phys. Lett.* **2005**, *404*, 232.

[16] Croce, A. E. *J. Fluorine Chem.* **1997**, *82*, 91.

[17] Basualdo, W. E.; Schumacher, H. J. *Z. Physik. Chem. NF*, **1965**, *47*, 57.

[18] Appelman, E. H.; Clyne, M. A. *J. Chem. Soc. Faraday Trans. I,* **1975**, *71*, 2072.

[19] Gambaruto, M; Sicre, J. E.; Schumacher, H. J. *J. Fluorine Chem.* **1975**, *5*, 175.

[20] King, G. W.; Santry, D. P.; Warren, C. H. *J. Mol. Spectrosc.,* **1969**, *32*, 108.

[21] Croce, A. E.; Cobos, C. J.; Castellano, E. *J. Photochem. Photobiol. A: Chem.* **1994**, *84,* 101.

[22] von Ellenrieder, G.; Schumacher, H. J. *Z. Physik. Chem. NF*, **1968**, *60*, 49.

[23] Croce de Cobos, A. E.; Cobos, C. J.; Castellano, E. *J. Phys. Chem.* **1989**, *93*, 274.

[24] Castellano, E; Schumacher, H. J. *Z. Physik. Chem. NF*, **1965**, *44*, 57.

[25] Dicelio, L; Schumacher, H. J. *An. Asoc. Quím. Argent. (This Journal),* **1978**, *66,* 283.

[26] Schack, C. J.; Christe, K. O.; *Inorg. Nucl. Chem. Lett.* **1978**, *14,* 293

[27] López, M. I.; Croce, A. E.; Sicre, J. E. *J. Photochem. Photobiol. A: Chem.* **1998**, *112,* 97.

[28] Carl, S. A.; Roehl, C. M.; Müller, R.; Moortgat, G. K.; Crowley, J. N. *J. Phys. Chem.* **1996**, *100,* 17191.

[29] Kukui, A; Roggenbuck, J.; Schindler, R. N. *Ber. Bunsenges. Phys. Chem.***1997***, 101,* 281.

[30] Cobos, C. J.; Croce, A. E.; Castellano, E.. *Chem. Phys. Lett.* **1997**, *266*, 253.
[31] Frisch, M. J.; Trucks, G. W.; Schlegel, H. B.; Scuseria, G. E.; Robb, M. A.; Cheeseman, J. R.; Montgomery, Jr., J. A.; Vreven, T.; Kudin, K. N.; Burant, J. C.; Millam, J. M.; Iyengar, S. S.; Tomasi, J.; Barone, V.; Mennucci, B.; Cossi, M.; Scalmani, G.; Rega, N.; Petersson, G. A.; Nakatsuji, H.; Hada, M.; Ehara, M.; Toyota, K.; Fukuda, R.; Hasegawa, J.; Ishida, M.; Nakajima, T.; Honda, Y.; Kitao, O.; Nakai, H.; Klene, M.; Li, X.; Knox, J. E.; Hratchian, H. P.; Cross, J. B.; Adamo, C.; Jaramillo, J.; Gomperts, R.; Stratmann, R. E.; Yazyev, O.; Austin, A. J.; Cammi, R.; Pomelli, C.; Ochterski, J. W.; Ayala, P. Y.; Morokuma, K.; Voth, G. A.; Salvador, P.; Dannenberg, J. J.; Zakrzewski, V. G.; Dapprich, S.; Daniels, A. D.; Strain, M. C.; Farkas, O.; Malick, D. K.; Rabuck, A. D.; Raghavachari, K.; Foresman, J. B.; Ortiz, J. V.; Cui, Q.; Baboul, A. G.; Clifford, S.; Cioslowski, J.; Stefanov, B. B.; Liu, G.; Liashenko, A.; Piskorz, P.; Komaromi, I.; Martin, R. L.; Fox, D. J.; Keith, T.; Al-Laham, M. A.; Peng, C. Y.; Nanayakkara, A.; Challacombe, M.; Gill, P. M. W.; Johnson, B.; Chen, W.; Wong, M. W.; Gonzalez, C.; Pople, J. A. Gaussian 03, Revision C.02, Gaussian, Inc., Pittsburgh PA, 2004.
[32] Becke, A. D. *J. Chem. Phys.*, **1983**, *98*, 5648.
[33] Becke, A. D. *Phys. Rev. A*, **1988**, *38,* 3098.
[34] Lee, C.; Yang, W.; Parr, R. G. *Phys. Rev. B*, **1988**, *37*, 785.
[35] Baboul, A. G.; Curtiss, L. A.; Redfern, P. C.; Raghavachari, K. *J. Chem. Phys.* **1999**, *110*, 7650.
[36] Sicre, J. E.; Cobos, C. J. *J. Mol. Struct. (Theochem),* **2003**, *620*, 215.
[37] Aubke, F.; Casper, B.; Müller, H. S. P.; Oberhammer, H.; Willner, H. *J. Mol. Struct.,* **1995**, *346*, 111.
[38] Jung, D.; Chen., C.-J, Bozzelli, J. W. H. *J. Phys. Chem. A,* **2000**, *104*, 9581.
[39] Anantharaman, B.; Melius, C. F. *J. Phys. Chem. A,* **2005**, *109*, 1734.
[40] Benson, S. W. *Chem. Rev.* **1978**, *78*, 23.
[41] Troe, J. *J. Phys. Chem. A,* **1979**, *83*, 114.
[42] Cobos, C. J.; Troe, J. *Z. Phys. Chem.* **2003**, *217*, 1031.
[43] Hippler, H. ; Troe, J; Wendelken H. J. *J. Chem. Phys.* **1983**, *78*, 6709.
[44] Troe, J. *J. Chem. Phys.* **1977**, *66*, 4745.
[45] Troe, J. *J. Chem. Phys.* **1977**, *66*, 4758.
[46] Nikitin, E. E. *Theor. Exp. Chem.* **1965** *1*, 144.
[47] Pechukas, P.; Light, J. C. *J. Chem. Phys.* **1965**, *42*, 3281.
[48] Cobos, C. J.; Troe, J. *J. Chem. Phys.* **1985**, *83*, 1010.
[49] Olzmann, M.; Troe, J. *Ber. Bunsenges. Phys. Chem.* **1992**, *96*, 1327.
[50] Badenes, M. P.; Croce, A. E.; Cobos, C. J. *J. Phys. Chem.*: A, DOI: 10.1021/jp054591x.